Effect of the nature of the metal on the breathing steps in MOFs with dynamic frameworks†

Franck Millange,*[a] Nathalie Guillou,[a] Richard I. Walton,[b] Jean-Marc Grenèche,[c] Irène Margiolaki[d] and Gérard Férey[a]

Received (in Cambridge, UK) 3rd June 2008, Accepted 25th July 2008
First published as an Advance Article on the web 5th September 2008
DOI: 10.1039/b809419e

The thermal behaviour of the nanoporous iron(III) terephthalate MIL-53 is in stark contrast to its chromium and aluminium analogues which show an expansion of the cell during dehydration; with iron, reversible dehydration occurs *via* evolution of the structure through a highly distorted metastable anhydrous phase to a more regular phase above 423 K in which pore volume remains approximately constant.

Among the most striking new families of materials discovered in the past few years are the open-framework metal–organic framework materials (MOFs).[1–4] The structures of these crystalline, hybrid solids are built up from metal coordination centres or oxy-clusters, linked by organic ligands to yield three-dimensional extended structures that often possess considerable porosity. Some of these MOFs show the largest surface areas known for crystalline solids (up to 6000 $m^2 g^{-1}$).[5,6] MOFs are now multifunctional materials with applications in separation and sorption that can rival traditional zeolite materials. This currently concerns hydrogen storage[7–10] and carbon dioxide storage[11,12] for energy and environmental purposes, but uses in other areas such as drug delivery,[13] catalysis[14] and electrode materials[15] are also emerging. The richness of MOFs relates to their easy tunability from micro- to mesoporous, by playing on the nature of the organic linker. The MIL-*n* family (MIL = Materials of Institut Lavoisier) illustrates these ideas well: by combining simple octahedral metal clusters with organic carboxylates a range of complex, porous structures are found, some of which exhibit a remarkable breathing property upon introduction of simple guest molecules, resulting in reversible expansion/contraction of unit cell volumes by hundreds of $Å^3$.[16–20] In this paper we describe a striking new example of this phenomenon, where the choice of the metal in the framework dramatically alters the behaviour of the solid.

MIL-53(Fe)_lt or $Fe^{III}(OH)\{O_2C\text{-}C_6H_4\text{-}CO_2\}\cdot H_2O$ was isolated as a phase-pure pale-orange crystalline powder under solvothermal conditions.‡ The material has analogies with Cr^{3+} and Al^{3+} materials MIL-53(Cr)[19,21] and MIL-53(Al)[22] but is not isostructural, as established from powder X-ray diffraction.‡ It is built up from corner-sharing *trans* chains of Fe octahedra linked by benzenedicarboxylate (BDC) moieties to form an open framework with one-dimensional channels running parallel to the *c*-axis. In the as-prepared hydrated form, the superstructure leads to two types of occluded water molecules that are located at the centre of two sets of diamond-shaped channels with similar sizes. Within each channel there are distinct types of water molecule: one channel contains a water molecule that is strongly hydrogen bonded to a partner of the same type generated by symmetry ($d_{Ow1\cdots Ow1}$ = 2.662 (1) Å) and also to an oxygen of the inorganic framework ($d_{O1\cdots Ow1}$ = 2.708 (1) Å), and in the other channel the water interacts weakly with its partner ($d_{Ow2\cdots Ow2}$ = 3.443 (1) Å), although it is also hydrogen bonded to a framework oxygen ($d_{O2\cdots Ow2}$ = 2.759 (1) Å).

The thermogravimetric analysis of **MIL-53(Fe)_lt** shows two weight losses of 6.97% (calc: 7.06%) below 333 K and 62.02% (calc: 61.62%) above 573 K corresponding to the departure of the occluded water molecules and the bound terephthalic acid, respectively, ultimately leading to decomposition of the phase at the highest temperature (supplementary information†). Variable-temperature powder X-ray diffraction studies, performed at up to 473 K under atmospheric pressure (Fig. 1), show that two major structural changes clearly occur upon dehydration, to produce finally the anhydrous $Fe^{III}(OH)\{O_2C\text{-}C_6H_4\text{-}CO_2\}$ or **MIL-53(Fe)_ht** above 423 K. At lower temperatures (323 K < T < 413 K), a triclinic metastable anhydrous phase **MIL-53(Fe)_int** is observed. The hydration–dehydration process is reversible and reproducible as shown in Fig. 1.

Fig. 2 compares the structures of the three MIL-53(Fe) materials to those of the two related MIL-53(Cr) materials.[19,21] MIL-53(Cr) shows a hydrated phase with contracted pores and a dehydrated phase with open pores, corresponding to an expansion of the unit cell volume by around 483 $Å^3$. In contrast, the loss of water from **MIL-53(Fe)_lt** results in a closing of the structure to form the metastable anhydrous phase **MIL-53(Fe)_int**, followed by a further small opening of the structure to obtain **MIL-53(Fe)_ht**. The volume change during the dehydration/rehydration of MIL-53(Fe) is actually rather small, around 87 $Å^3$. Further proof that the intermediate phase is fully dehydrated was provided by heating a sample at

---

[a] *Institut Lavoisier (UMR CNRS 8180), Université de Versailles St-Quentin en Yvelines, 45 Avenue des Etats-Unis, 78035 Versailles Cedex, France. E-mail: franck.millange@uvsq.fr; Fax: (+33) 1-3925-4358; Tel: (+33) 1-3925-4361*
[b] *Department of Chemistry, University of Warwick, Coventry, UK CV4 7AL*
[c] *Laboratoire de Physique de l'Etat Condensé (UMR CNRS 6087), Université du Maine, 72085 Le Mans Cedex, France*
[d] *ID31, Materials Science Group, European Synchrotron Radiation Facility, BP 220, 38043 Grenoble Cedex, France*

† Electronic supplementary information (ESI) available: Thermogravimetric data and refined crystallographic parameters. CCDC reference numbers 690314–690316. For ESI and crystallographic data in electronic format see DOI: 10.1039/b809419e

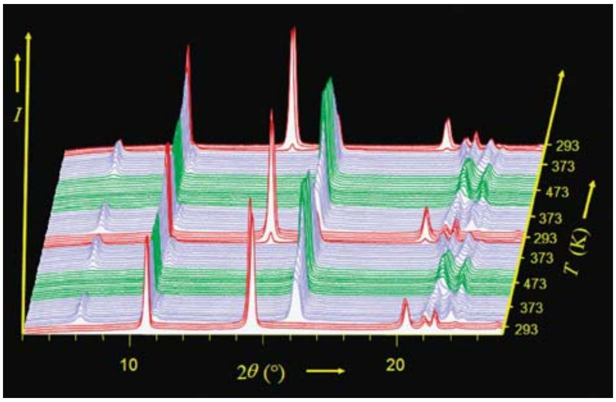

Fig. 1 Thermal evolution of diffractograms during dehydration–hydration process. Red: **MIL-53(Fe)_lt**; blue: **MIL-53(Fe)_int**; green: **MIL-53(Fe)_ht**.

523 K in a quartz capillary for 24 h, sealing under dry air: then the high resolution powder XRD measured at room temperature is consistent with the presence of only **MIL-53(Fe)_int**.

The topologies of the hydrous phase and the intermediate metastable phase are identical to that of the final anhydrous material, but the lower symmetry means that there are two sets of diamond-shaped channels with different sizes. These can be described in terms of iron–iron distances within each structure. The distances between two nearest iron(III) cations along the *c*-axis (small diagonal of the lozenge) in **MIL-53(Fe)_lt** are Fe$_1$–Fe$_1$ = 7.353 Å and Fe$_1$–Fe$_1$ = 7.702 Å in the largest diamond-shaped tunnel while the distances are Fe$_2$–Fe$_3$ = 7.518 Å in the smallest channel. In comparison, the distances between two nearest iron(III) cations along the *a*-axis (small diagonal of the lozenge) in **MIL-53(Fe)_int** are Fe$_2$–Fe$_2$ = 7.762 Å and Fe$_1$–Fe$_1$ = 7.499 Å in the largest diamond-shaped tunnel while the distances are Fe$_2$–Fe$_2$ = 5.723 Å and Fe$_1$–Fe$_1$ = 5.993 Å in the smallest channel. For **MIL-53(Fe)_ht** the unique Fe–Fe distance is 6.759 Å.

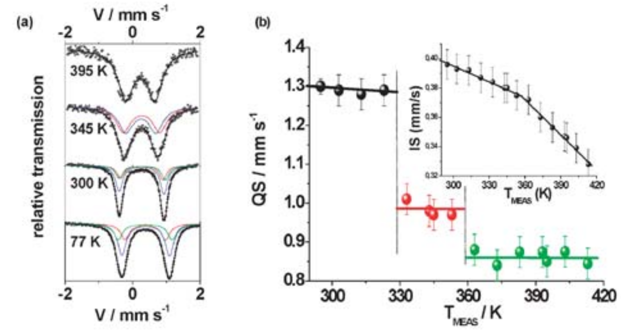

Fig. 3 (a) Representative *in situ* Mössbauer spectra and (b) temperature dependence of the mean quadrupolar splitting and mean isomer shift (inset).

Further evidence for the structural changes accompanying the dehydration process is provided by *in situ* ^{57}Fe transmission Mössbauer spectra recorded from samples held in a custom-built cryofurnace under room pressure, as illustrated in Fig. 3. The quadrupolar hyperfine structures allow three different temperature regimes to be distinguished: these different profiles may be fitted by one quadrupole broadened line component at temperatures from 77 K to 333 K, two quadrupolar components from 333 K to 363 K (with two slightly different quadrupolar splitting values) and one quadrupolar component from 363 K up to 423 K. The low temperature regime spectra are in fact better described by

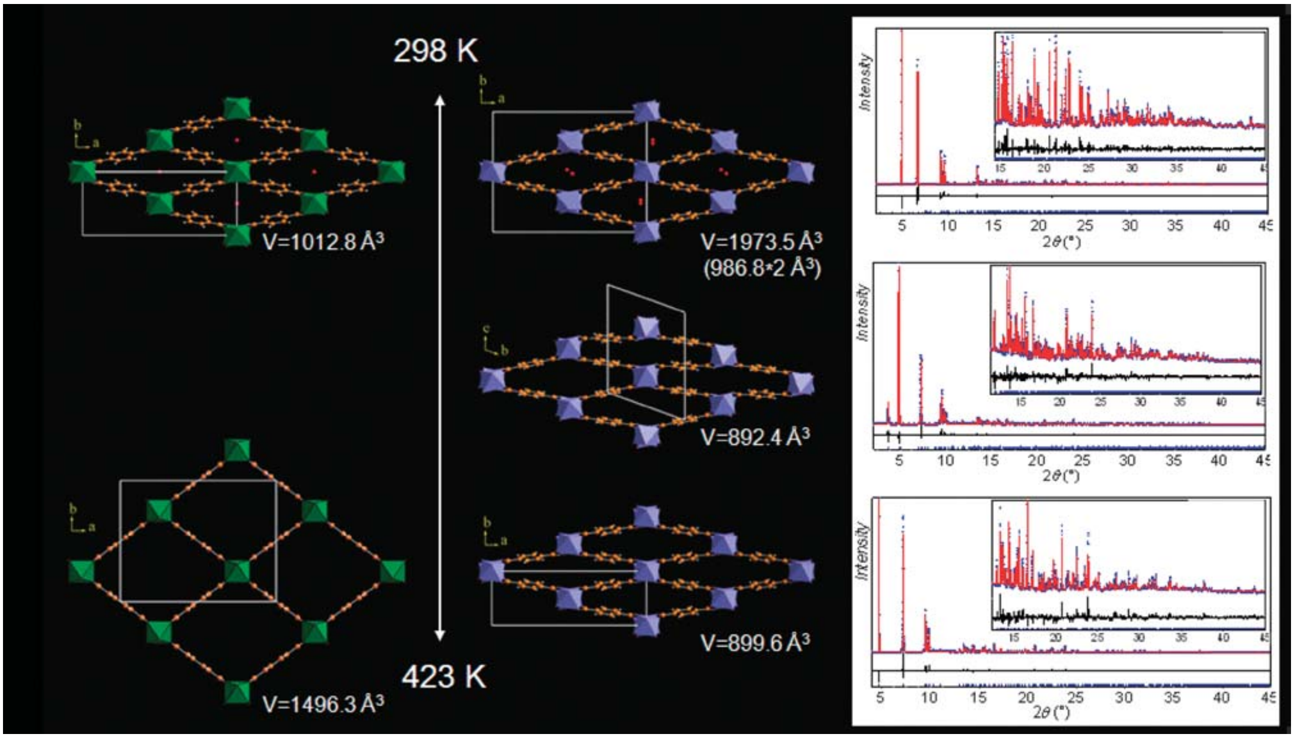

Fig. 2 Left: Crystal structures of the hydrated and anhydrous chromium phases. Middle: Crystal structures of the hydrated (lt), intermediate anhydrous (int) and anhydrous (ht) iron phases. Right: Final Rietveld refinements of the three iron dicarboxylates.

three quadrupolar components with absorption ratio 2 : 1 : 1, in agreement with powder diffraction results. The isomer shift values suggest that the octahedral coordination of ferric ions in a high-spin state is maintained over all temperatures, while those of the quadrupolar splitting demonstrate that the local environment of the metal is subject to small changes in bond distances/angles upon dehydration. The temperature dependence of the quadrupolar splitting is clearly consistent with two structural phase transitions which can be matched to the departure of structural water molecules and then the transformation from intermediate anhydrous into final anhydrous phase (Fig. 3(b)). The three regimes show evidence for the presence of three Fe(III) sites, then two different Fe(III) sites and then a single Fe(III) site, consistent with the structures determined by powder diffraction. The shift of transition temperature is due to the instrumental conditions (each Mössbauer spectrum requires about 12 h acquisition time while each X-ray pattern is obtained in 30 min). The reversibility of these phase transitions has also been checked by *in situ* cooling. The two observed temperature dependences of isomer shift are due to the change of local electronic density attributed to the departure of water molecules.

It is difficult to find reasons for such a striking change in behaviour between **MIL-53(Cr)** and **MIL-53(Fe)**. Despite the similar ionic radii and electronegativities of Cr^{3+} and Fe^{3+} the materials show a very different response towards a simple guest molecule such as water. The bond distances within the octahedral building units are rather similar in each case (for **MIL-53(Fe)_lt** $Fe–O_{av} = 2.00$ Å, for **MIL-53(Fe)_int**, $Fe–O_{av} = 2.00$ Å and for **MIL-53(Fe)_ht**, $Fe–O_{av} = 1.99$ Å and for **MIL-53(Cr)_lt**, $Cr–O_{av} = 1.99$ Å). The M–O–M chains are disrupted very little upon hydration–dehydration and small changes in the relative orientation of the terephthalate linkers could be responsible for the behaviour of the framework structure upon hydration. The dramatically different dehydration/hydration behaviour of a MOF material depending on the identity of the framework metal suggests that this might be a subtle means of modifying the properties of these materials for practical application. Studies of the sorption and separation properties of these materials[23] and how they are affected by the choice of metal are now underway. Preliminary results have already shown that the CO_2 sorption is very different between **MIL-53(Fe)** and **MIL-53(Cr)**, for example.

This work was supported by CNRS, EU funding *via* FP6-Specific Targeted Research Project "DeSANNS" and French ANR "CONDMOFs" funding.

Notes and references

‡ **MIL-53(Fe)_lt** was solvothermally synthesised as previously described.[15] Quantitative elemental analyses gave the following results: Fe: 23.7%; C: 35.6%; H: 2.68% and F: 1.31% which compare well with those calculated from the formula $Fe^{III}(OH)(O_2C\text{-}C_6H_4\text{-}CO_2)\cdot(H_2O)$: Fe: 21.9%; C: 37.6%; H: 2.68% and F: 1.48%. Powder X-ray diffraction data were collected on ID31 of the ESRF from powdered samples contained in a 1 mm diameter quartz capillary. The beamline receives X-rays from the synchrotron source (which operates with an average energy of 6 GeV and a current beam of typically 100 mA) from an undulator device. The incident X-ray wavelength was 0.79989667 Å using an incident beam size of 2.0 mm (horizontal) × 1.0 mm (vertical). The sample was rapidly spun during data collection to ensure good powder averaging. Extractions of the peak positions, pattern indexing and Rietveld refinements were carried out with the TOPAS program.[24]

1 G. Férey, *Chem. Soc. Rev.*, 2008, **37**, 191.
2 G. Férey, C. Mellot-Draznieks, C. Serre and F. Millange, *Acc. Chem. Res.*, 2005, **38**, 217.
3 S. Kitagawa, S. Noro and T. Nakamura, *Chem. Commun.*, 2006, 701.
4 O. M. Yaghi, M. O'Keefe, H. K. Ockwig, M. Chae and M. Eddaoudi, *Nature*, 2003, **423**, 705.
5 H. K. Chae, D. Y. Siberio-Pérez, J. Kim, Y. Go, M. Eddaoudi, A. J. Matzger, M. O'Keeffe and O. M. Yaghi, *Nature*, 2004, **427**, 523.
6 G. Férey, C. Mellot-Draznieks, C. Serre, F. Millange, J. Dutour, S. Surble and I. Margiolaki, *Science*, 2005, **309**, 2040.
7 M. Latroche, S. Surblé, C. Serre, C. Mellot-Draznieks, P. L. Llewellyn, J.-H. Lee, J.-S. Chang, H. J. Sung and G. Férey, *Angew. Chem., Int. Ed.*, 2006, **45**, 8227.
8 X. Lin, J. Jia, P. Hubberstey, M. Schröder and N. R. Champness, *CrystEngComm*, 2007, **9**, 438.
9 N. L. Rosi, J. Eckert, M. Eddaoudi, D. T. Vodak, J. Kim, M. O'Keeffe and O. M. Yaghi, *Science*, 2003, **300**, 1127.
10 X. Zhao, B. Xiao, A. J. Fletcher, K. M. Thomas, D. Bradshaw and M. J. Rosseinsky, *Science*, 2004, **306**, 1012.
11 S. Bourrelly, P. L. Llewellyn, C. Serre, F. Millange, T. Loiseau and G. Férey, *J. Am. Chem. Soc.*, 2005, **127**, 13519.
12 A. R. Millward and O. M. Yaghi, *J. Am. Chem. Soc.*, 2005, **127**, 17998.
13 P. Horcajada, C. Serre, M. Vallet-Regi, M. Sebban, F. Taulelle and G. Férey, *Angew. Chem., Int. Ed.*, 2006, **45**, 5974.
14 P. Horcajada, S. Surble, C. Serre, D. Y. Hong, Y. K. Seo, J. S. Chang, J. M. Greneche, I. Margiolaki and G. Férey, *Chem. Commun.*, 2007, 2820.
15 G. Férey, F. Millange, M. Morcrette, C. Serre, M. L. Doublet, J. M. Grenèche and J. M. Tarascon, *Angew. Chem., Int. Ed.*, 2007, **46**, 3259.
16 K. Barthelet, J. Marrot, D. Riou and G. Férey, *Angew. Chem., Int. Ed.*, 2002, **41**, 281.
17 N. A. Ramsahye, G. Maurin, S. Bourrelly, P. L. Llewellyn, T. Loiseau, C. Serre and G. Férey, *Chem. Commun.*, 2007, 3261.
18 C. Serre, C. Mellot-Draznieks, S. Surblé, N. Audebrand, Y. Filinchuk and G. Férey, *Science*, 2007, **315**, 1828.
19 C. Serre, F. Millange, C. Thouvenot, M. Nogues, G. Marsolier, D. Louer and G. Férey, *J. Am. Chem. Soc.*, 2002, **124**, 13519.
20 K. Uemura, R. Matsuda and S. Kitagawa, *J. Solid State Chem.*, 2005, **178**, 2420.
21 F. Millange, C. Serre and G. Férey, *Chem. Commun.*, 2002, 822.
22 T. Loiseau, C. Serre, C. Huguenard, G. Fink, F. Taulelle, M. Henry, T. Bataille and G. Férey, *Chem.–Eur. J.*, 2004, **10**, 1373.
23 F. Millange, N. Guillou, C. Serre, G. Férey and R. I. Walton, *Angew. Chem., Int. Ed.*, 2008, **47**, 4100.
24 *TOPAS V3.0: General Profile and Structure Analysis Software for Powder Diffraction Data*, Bruker AXS Ltd, 2004.